Cardiovascular Research (2009) **84**, 317–325
doi:10.1093/cvr/cvp215

Bone marrow-derived cells do not repair endothelium in a mouse model of chronic endothelial cell dysfunction

Tashera E. Perry[1†], Minjung Song[1†], Daryl J. Despres[2], Soo Mi Kim[3], Hong San[4], Zu-Xi Yu[5], Nalini Raghavachari[6], Jurgen Schnermann[3], Richard O. Cannon III[1], and Donald Orlic[1*]

[1]*Translational Medicine Branch, National Heart, Lung, and Blood Institute, National Institutes of Health, 9000 Rockville Pike, Building 10-CRC, Room 6-3130, Bethesda, MD 20892, USA;* [2]*Mouse Imaging Facility, National Institute of Neurological Disorders and Stroke, National Institutes of Health, Bethesda, MD, USA;* [3]*Kidney Disease Branch, National Institute of Diabetes and Digestive and Kidney Disease, National Institutes of Health, Bethesda, MD, USA;* [4]*Genome Technology, National Human Genome Research Institute, National Institutes of Health, Bethesda, MD, USA;* [5]*Pathology Core, National Heart, Lung, and Blood Institute, National Institutes of Health, Bethesda, MD, USA; and* [6]*Gene Expression Core, National Heart, Lung, and Blood Institute, National Institutes of Health, Bethesda, MD, USA*

Received 27 January 2009; revised 17 June 2009; accepted 18 June 2009; online publish-ahead-of-print 3 July 2009

Time for primary review: 29 days

KEYWORDS
Stem cells;
Bone marrow transplantation;
Endothelial NOS deficiency;
Hypertension

Aims Bone marrow (BM)-derived endothelial progenitor cells (EPCs) in the circulation replace damaged vascular endothelium. We assessed the hypothesis that a BM transplant from healthy animals would restore normal arterial endothelium and prevent hypertension in young endothelial nitric oxide synthase-deficient ($eNOS^{-/-}$) mice.
Methods and results Radiation or busulfan-induced BM ablation in $eNOS^{-/-}$ mice on day 6, day 14, or day 28 was followed by a BM transplant consisting of enhanced green fluorescent protein positive ($EGFP^{+}$) cells from C57BL/6J mice. Peripheral blood cell chimerism was always greater than 85% at 4 months after BM transplant. Molecular assays of heart, kidney, and liver revealed low-level chimerism in all treatment groups, consistent with residual circulating $EGFP^{+}$ blood cells. When aorta, coronary, renal, hepatic, and splenic arteries in BM-transplanted $eNOS^{-/-}$ mice were examined by confocal microscopy, there were no EGFP- or eNOS-positive endothelial cells detected in these vessels in any of the treatment groups. Likewise, telemetry did not detect any reduction in blood pressure. Thus, no differences were observed in our measurements using several different treatment protocols.
Conclusion We found no evidence for BM-derived EPC renewal of endothelium in this eNOS-deficient mouse model of a chronic vascular disease or in wild-type mice during postnatal growth. Hence, renewal of chronic dysfunctional endothelium and endothelial homeostasis may be dependent on resident vascular progenitor cells.

1. Introduction

Recent evidence indicates that a population of progenitor cells that exist in the circulation has the potential to repair endothelium and maintain angiogenesis during postnatal life. In human subjects, these cells, termed endothelial progenitor cells (EPCs), can be mobilized in large numbers from bone marrow (BM) by a single injection of AMD3100, a CXCR4 antagonist,[1] and their number in blood has been reported to correlate directly with vascular endothelial function when measured by flow-mediated brachial artery reactivity.[2]

In animal studies, BM-derived EPCs contribute to recovery of the vascular system in response to tissue ischaemia resulting from intra-arterial trauma or arterial ligation.[3–7] Following mobilization into the circulation, EPCs are recruited to the traumatized or ischaemic tissues in response to secretion of stromal cell-derived factor-1,[8,9] or vascular endothelial growth factor.[10] Likewise, infusion of BM-derived mononuclear cells into an acutely ischaemic hind-limb in mice

* Corresponding author. Tel: +1 301 402 0903; fax: +1 301 402 0888.
E-mail address: dorlic@nhlbi.nih.gov
†These two authors contributed equally to this study.

increases local reperfusion.[11,12] Data from these and other studies support the concept that a subpopulation of BM cells promote vascular repair in acute injuries.[13,14]

Whereas previous animal studies have relied mainly on acute injury to demonstrate the contribution of BM-derived EPCs to vascular biology, our investigation focused on whether EPCs can replace dysfunctional endothelium in a setting of chronic vascular disease. We hypothesized that progenitor cells may be recruited from BM over time in response to the chronic hypertension observed in endothelial nitric oxide synthase-deficient ($eNOS^{-/-}$) mice.[15] Further, we anticipated that early transplantation of enhanced green fluorescent protein positive ($EGFP^{+}$), $eNOS^{+}$ BM cells into day-6 and day-14 neonates and day-28 young adult mice might facilitate incorporation of donor-derived progenitor cells into the expanding cardiovascular system. We did not find evidence for incorporation of any donor-derived $EGFP^{+}$ $eNOS^{+}$ progenitor cells into the endothelium of conducting arteries and arterioles, or prevention of hypertension. Our study suggests that endothelial renewal in homeostasis and in chronic dysfunctional states is dependent upon progenitor cells that reside in or near the arterial wall.

2. Methods

2.1 Animal model

All mice were obtained from Jackson Laboratories, Bar Harbor, ME, USA. Enhanced GFP^{+} C57BL/6-Tg(UBC_GFP)30Scha/J mice were used as donors for BM transplantation in B6.129P2-Nos3tm1Unc/J $eNOS^{-/-}$ mice. The investigation conforms to the *Guide for the Care and Use of Laboratory Animals* published by the US National Institutes of Health (NIH Publication No.85-23, revised 1996). All animals were handled following the guidelines of the Animal Care and Use Committee at the NHLBI, National Institutes of Health (Animal Study Proposal H-0162).

2.2 Bone marrow harvest and transplantation

BM cells were harvested from the femurs and tibias of 2–4 month old $EGFP^{+}$ donor mice and the nucleated cells were enriched by lysing red blood cells with ACK buffer (Cambrex, Walkersville, MD, USA). Total body sub-lethal radiation (6 Gy) was administered to day-6, day-14, and day-28 $eNOS^{-/-}$ mice and 6 h later $2.5–3.0 \times 10^{7}$ $EGFP^{+}$ BM nucleated cells were injected intraperitoneally into day 6 and day 14 neonates or intravenously into day-28 young adult mice. Non-treated transgenic $EGFP^{+}$ mice and wild-type (WT) mice transplanted with $EGFP^{+}$ BM served as controls. There were 12 mice studied in these three experimental groups and 8 mice in the two control groups. In an additional series of experiments, to counter any possibility that lasting radiation-induced damage might prevent arterial endothelium from responding to signals that govern endothelial repair, we performed experiments using the myeloablative agent busulfan. A single dose of busulfan was administered to three day-13 and three day-27 mice at a dose of 20 gm/kg body weight. BM was transplanted 1 day later.

2.3 Cardiac ultrasound

Echocardiography was performed using the VisualSonics' Vevo 770® (VisualSonics, Inc., Toronto, Ontario, Canada) equipped with a 15 MHz probe on mice at 4 months post-BM transplant and on age-matched WT and $eNOS^{-/-}$ controls. Mice were kept under light sedation with 1–2% isoflurane for the duration of the imaging session. Images were obtained from short- and long-axis views of the left ventricle. Two-dimensional and M-mode echocardiography images were observed. Cardiac structures such as the thickness of the interventricular septum and posterior wall, and the diameter of the left ventricle were measured based on M-mode images, and functional features [fractional shortening (FS), ejection fraction (EF), cardiac output (CO), and stroke volume (SV)] were automatically calculated with Vevo 770® software from structural values.

2.4 Flow cytometry

Blood was collected from the retro-orbital sinus of BM-transplanted $eNOS^{-/-}$ recipient mice at 4 months post-transplant. Red blood cells were lysed in ACK buffer and the remaining nucleated blood cells were washed in phosphate-buffered saline (PBS) and analysed for EGFP fluorescence using a fluorescence-activated cell sorter (Calibur Instrument, BD Biosciences, San Jose, CA, USA). All BM-transplanted $eNOS^{-/-}$ mice selected for further study showed $>85\%$ chimerism at 4 months after transplantation.

2.5 Blood pressure monitoring

Blood pressure was measured in BM-transplanted $eNOS^{-/-}$ mice, non-transplanted $eNOS^{-/-}$ controls, and WT controls by radiotelemetry (Data Sciences International, St Paul, MN, USA). For implantation of PA-C10 pressure transmitters, mice were anesthetized with an intraperitoneal injection of 90 mg/kg ketamine and 10 mg/kg xylazine. The catheter was inserted through the left carotid artery into the aortic arch with the transmitter body tucked into a subcutaneous pocket of the right flank. Mice were returned to their cages the day after surgery, and were observed for 7–10 days before the initial recordings. Mice had access to food and water at all times, and the recording room was maintained at an ambient temperature of 21–22°C with a 12 h light/dark cycle. The transmitter signal was captured using the RPC-1 receiver, a 20 channel data exchange matrix, APR-1 ambient pressure monitor, and a Data Quest ART Silver 2.3 acquisition system (Data Sciences International). Mean arterial pressure, systolic blood pressure, diastolic blood pressure, pulse pressure, heart rate, and activity values were recorded for 10 s at 2 min intervals and hourly averages were calculated for each mouse during a period of 100 consecutive hours. The mean $\pm$ SD was calculated for 17 WT control mice, 4 non-treated $eNOS^{-/-}$ control mice, and 4 BM-transplanted $eNOS^{-/-}$ mice.

2.6 Western blot

Total protein from heart, kidney, and spleen was extracted using a steel homogenizer ball (Restch, Newtown, PA, USA). Extracted protein concentrations were determined by the bicinchoninic acid (BCA) protein assay (Pierce, Rockford, IL, USA). Protein samples (20 μg) were resolved on a 4–20% Novex® Tris-Glycine gel (Invitrogen, Carlsbad, CA, USA) and transferred to a nitrocellulose membrane (Invitrogen) using an iBlot™ Dry Blotting system (Invitrogen). The membrane was blocked with 5% skim milk in PBS for 1 h at room temperature. Primary antibodies were rabbit anti-EGFP (1:10,000, Invitrogen) and mouse anti-glyceraldehyde-3-phosphate dehydrogenase (GAPDH; 1:500, Imgenex, San Diego, CA, USA). The membrane was exposed to the primary antibodies overnight at 4°C, followed by three 5 min washes with Tris-buffered saline containing 0.05% Tween 20. After washing, the membrane was incubated with horseradish peroxidase conjugated goat anti-rabbit or anti-mouse antibodies (Pierce) for 2 h at room temperature. Enhanced chemiluminescence reaction was performed using a SuperSignal® West Femto enhancer kit (Pierce), according to the manufacturer's instructions.

2.7 Quantitative RT—PCR

Total RNA was isolated from kidney, liver, and spleen and preserved in RNAlater buffer (Ambion, Austin, TX, USA) following the manufacturer's protocol in the RNeasy Mini Kit (Qiagen, Valencia, CA, USA).

Reverse transcription was performed on the GeneAmp PCR System 9700 (Applied Biosystems, Foster City, CA, USA) using the SuperScript II RT–PCR Kit (Invitrogen). PCR was performed on the ABI Prism 7000 using TaqMan Universal PCR Master Mix and Assays-on-Demand Gene Expression probes (Applied Biosystems) specific for eNOS, EGFP, and ß-actin. Relative eNOS and EGFP mRNA levels were calculated using a $2^{\Delta\Delta}$Ct method.

2.8 DNA electrophoresis

Heart, kidney, and spleen were obtained for DNA analysis. DNA was isolated following the manufacturer's protocol for the DNeasy Tissue Kit (Qiagen) and amplified with primers specific for eNOS and EGFP on the GeneAmp PCR System 9700 (Applied Biosystems). To detect eNOS, DNA was amplified in Platinum Blue PCR SuperMix (Invitrogen) with forward 5′-ATTTCCTGTCCCCTGCCTTC-3′, and reverse primers 5′-GGCCAGTCTCAGAGCCATAC-3′, and primer specific for the neomycin-resistance gene insert 5′-TGGCTACCCGTGATATTGCT-3′. These primers were designed to produce a 450 bp band consisting of amplicons of the WT *eNOS* gene and a 500 bp band representing amplicons consisting of 450 bp of the disrupted exon 12 of the *eNOS* gene plus 50 bp of the targeting construct. To detect EGFP, DNA was amplified using a HotStar *Taq* Polymerase Kit (Qiagen) with primers 5′-AAGTTCATCTGCACCACCG-3′ and 5′-TCCTTGAAGAA GATGGTGCG-3′ that generate a 200 bp product. Glyceraldehyde 3-phosphate dehydrogenase (GAPDH) (250 bp) was used as a loading control. DNA bands were isolated in 2% agarose gels.

2.9 Immunohistochemistry and confocal microscopy

Tissues were fixed in 4% formaldehyde and 5 μm paraffin sections were prepared (HistoServ, Germantown, MD, USA). Rehydrated paraffin sections were submerged in boiling citrate buffer at pH 6.0 for 15 min in a microwave oven. Sections were allowed to cool in citrate buffer for 30 min at room temperature. After washing, sections were incubated with primary antibody for 1 h at 37°C in a moist chamber. We used the following antibodies: goat polyclonal to EGFP (ab5450); rabbit polyclonal to smooth muscle alpha actin (SMαA) (ab5694); rabbit polyclonal to von Willebrand Factor (vWF) (ab6994) all from Abcam, Cambridge, MA, USA, and rabbit polyclonal to NOS3 (eNOS) (sc-654) from Santa Cruz Biotechnology, Inc., Santa Cruz, CA, USA. Negative controls were not exposed to primary antibody. After washing, sections were incubated with secondary antibody conjugated to fluorescein isothiocyanate or Texas Red for 1 h at 37°C in a moist chamber and then mounted with Vectashield containing 4′,6-diamidino-2-phenylindole (DAPI) a stain for DNA. Images were obtained using a confocal microscope (Leica SP1; Leica Microsystems, Heidelberg, Germany) equipped with an Ar/Kr/HeNe laser combination. Photographs were taken with Leica confocal software. For controls, there were five EGFP$^+$ mice and three WT mice that were BM-transplanted on day 28. Experimental mice included 12 eNOS$^{-/-}$ mice in three categories of radiation treatment: five were irradiated and transplanted on day 6, two were transplanted on day 14, and five on day 28. In addition, three eNOS$^{-/-}$ mice were myeloablated with busulfan on day 13 and transplanted on day 14, and three were myeloablated on day 27 and transplanted on day 28. All forms of treatment resulted in comparable high-level reconstitution of splenic and medullary haematopoiesis and no incorporation of donor cells into arterial endothelium. For each animal we fixed and embedded a portion of heart, kidney, liver, and spleen, and for some we also examined aorta, lung, small intestine, skin, and skeletal muscle. Heart, kidney, liver, and spleen from each mouse were embedded in one block and from each block, five or more slides (range 5–14, total of 124 slides) were prepared. Two sections, each 5 μm thick, were mounted per slide. One section was stained for EGFP and either SMαA, vWF, or eNOS and examined for donor cell incorporation into arterial endothelium. The other section served as a negative control and was stained only with secondary antibodies. For each organ on each slide, we examined one or more large conduit arteries and 5–20 arterioles for incorporation of EGFP$^+$ endothelial cells.

2.10 Statistical analysis

GraphPad Prism 4 (GraphPad Software, Inc., San Diego, CA, USA) was used to calculate one-way analyses of variance (ANOVA). When $P < 0.05$, Tukey's multiple comparison *post hoc* tests were performed to determine the source of variance ($P < 0.05$). When calculating data from qRT–PCR for eNOS and EGFP expression, unpaired, independent Student's *t*-test was performed to obtain *P*-values. In addition, Student's *t*-test was performed to calculate *P*-values using an EXCEL program (Microsoft 2003).

3. Results

3.1 Chimerism in transplanted mice

Chimerism in transplanted eNOS$^{-/-}$ mice was determined by the percentage of EGFP$^+$ nucleated blood cells found in peripheral blood at 4 months post-transplant (*Figure 1A*). Mice showing greater than 85% chimerism were used for further study.

3.2 Body weight

Body weight for BM-transplanted eNOS$^{-/-}$ mice and non-BM-transplanted eNOS$^{-/-}$ control mice was obtained to ascertain possible effects of treatment on growth and development. Mice in the non-transplanted eNOS$^{-/-}$ control group (20 ± 1 gm) and in the BM-transplanted eNOS$^{-/-}$ group (21 ± 1 gm) had significantly lower body weight than WT mice (24 ± 1 gm) ($P < 0.05$). The BM-transplanted eNOS$^{-/-}$ group showed a small but not significant increase in weight compared with the eNOS$^{-/-}$ control group.

3.3 Cardiac structure and function

Cardiac ultrasound was performed on WT, non-transplanted eNOS$^{-/-}$ age-matched controls and BM-transplanted mice at 4 months post-transplantation to observe any changes in cardiac structures or functions resulting from procedures associated with the BM transplant (Supplementary material online, *Table S1*). Control eNOS$^{-/-}$ mice and BM-transplanted eNOS$^{-/-}$ mice exhibited a decreased thickness of the interventricular septum in diastole (IVSd) and systole (IVSs) compared with WT controls ($P < 0.05$). However, left ventricle posterior wall thickness was comparable among all three groups. Likewise, the left ventricle internal diameter in eNOS$^{-/-}$ controls and BM-transplanted eNOS$^{-/-}$ mice did not differ in diastole and systole compared with WT control mice. Cardiac functions such as FS, SV, EF, and CO obtained for WT controls, eNOS$^{-/-}$ mice, and BM-transplanted eNOS$^{-/-}$ mice were not significantly different.

3.4 Blood pressure monitoring

Blood pressure transmitters with a catheter implanted in the aortic arch were used to record mean arterial pressure, pulse pressure, heart rate, systolic and diastolic blood pressure, and activity of age-matched WT controls, BM-transplanted eNOS$^{-/-}$ mice and non-transplanted eNOS$^{-/-}$ controls (*Figure 1B*). Heart rate was significantly

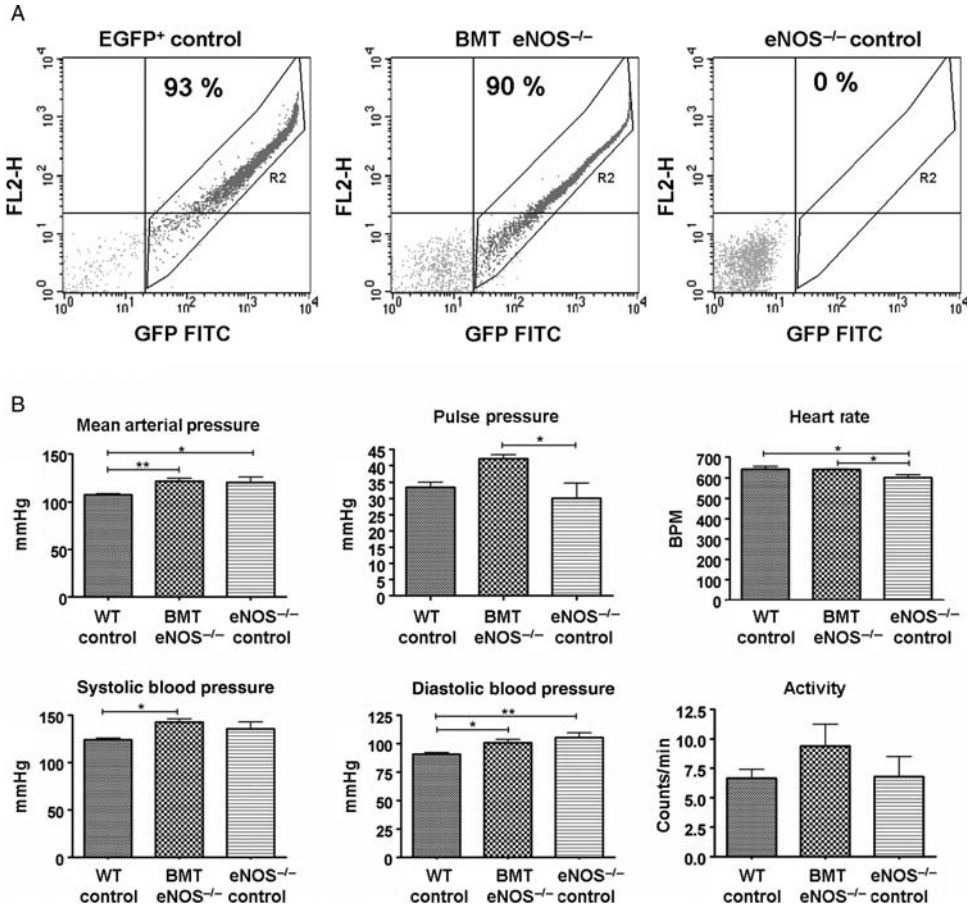

Figure 1 (*A*) Circulating white blood cells were analysed by flow cytometry to determine the percent chimerism. (*B*) Haemodynamic parameters were assessed 4 months after BM transplantation and in age-matched controls by telemetry. Activity measures lateral movement. Heart rate and pulse pressure were increased in BM-transplanted eNOS$^{-/-}$ mice vs. eNOS$^{-/-}$ controls. Mean $\pm$ SD. *$P < 0.05$, **$P<0.01$.

lower in untreated eNOS$^{-/-}$ mice compared with WT controls (602 ± 15 and 642 ± 4 bpm, respectively, $P < 0.05$), but was improved in eNOS$^{-/-}$ mice following BM transplantation (642 ± 14). No significant differences in mean arterial pressure or systolic and diastolic blood pressure were observed between untreated eNOS$^{-/-}$ and BM-transplanted eNOS$^{-/-}$ mice. In addition, there were no differences in activity levels, assessed by lateral body movements over a consecutive 100 h period, between BM-transplanted and control groups suggesting that no apparent harmful effect resulted from radiation, busulfan, and BM transplant procedures.

3.5 Enhanced green fluorescent protein positive expression

High-level EGFP expression was detected by western blot analysis in tissue lysates from heart, kidney, and spleen obtained from transgenic EGFP control mice. Corresponding tissues from untreated eNOS$^{-/-}$ mice were negative. The heart and kidney from BM-transplanted eNOS$^{-/-}$ mice displayed low quantities of donor-derived EGFP (*Figure 2A* and *B*). When values for EGFP transgenic mouse heart and kidney were normalized to 1.0, we observed a three- to four-fold greater band intensity in these mice compared with BM-transplanted eNOS$^{-/-}$ mice. The spleens in BM-transplanted eNOS$^{-/-}$ mice expressed high levels of EGFP because their haematopoietic tissue was fully reconstituted by EGFP^{+} donor cells.

3.6 DNA and mRNA analysis

DNA electrophoresis was performed on homogenates of heart, kidney, and spleen from day-6, day-14 and day-28 BM-transplanted eNOS$^{-/-}$ mice. Banding patterns showed trace quantities of WT eNOS (450 bp) in heart and kidney of BM-transplanted eNOS$^{-/-}$ mice, whereas large quantities of DNA encoding WT eNOS were observed in the spleens of these mice (*Figure 2C*). The 500 bp band consisted of 450 bp of exon 12 of the disrupted *eNOS* gene plus 50 bp of the targeting construct. A similar pattern emerged for EGFP DNA analysis (*Figure 2D*). The level of mRNA expression in kidney, liver, and spleen was quantified by RT–PCR using ß-actin as a loading control (*Figure 2E* and *F*). EGFP and eNOS mRNA was highly expressed in transgenic EGFP^{+} control tissues. Low levels of EGFP and WT eNOS expression in kidney and liver of BM-transplanted eNOS$^{-/-}$ mice were likely due to residual circulating EGFP^{+} donor-derived blood cells in these organs. In contrast to kidney and liver, the high-level expression of EGFP mRNA in the spleen of BM recipients resulted from donor cell reconstitution of the splenic haematopoietic tissue. As in kidney and liver, WT eNOS mRNA (*Figure 2F*) was low in spleen. Presumably, the EGFP^{+} blood cells in spleen did not express eNOS mRNA.

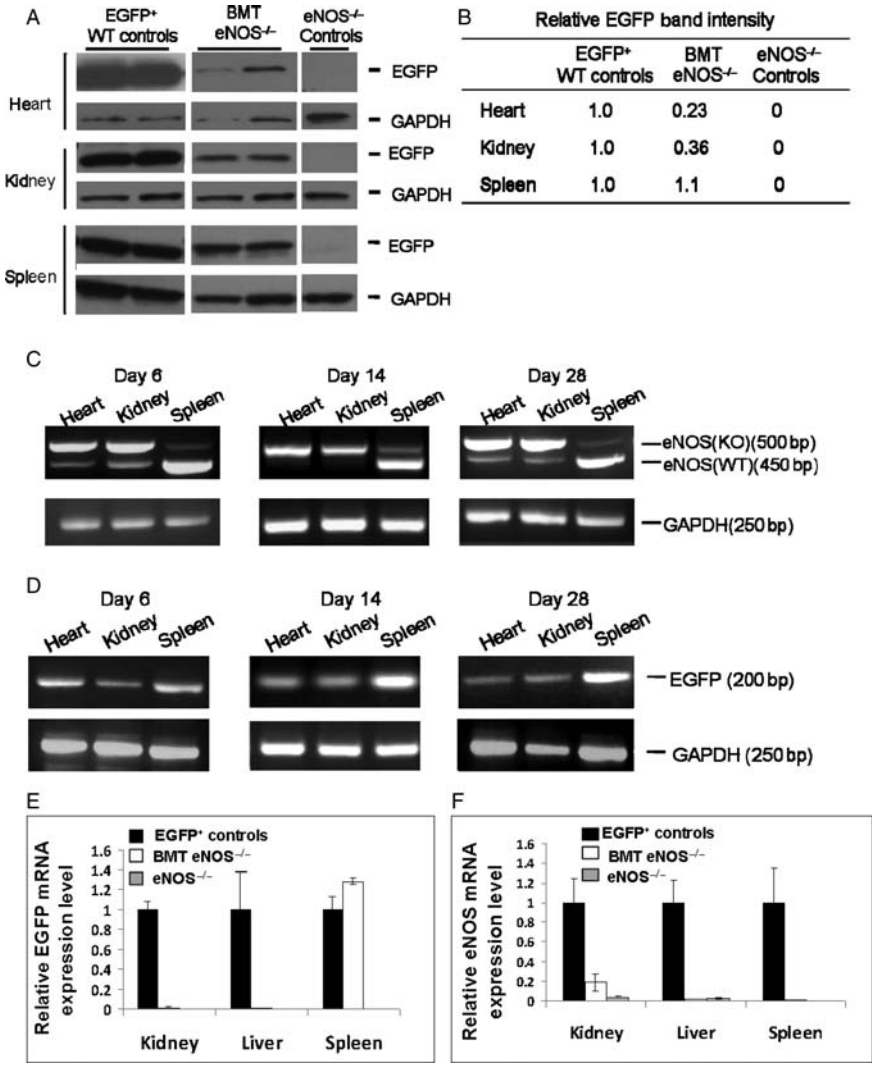

Figure 2 (*A*) EGFP expression was detected by western blot analysis in heart, kidney, and spleen of EGFP$^+$ controls and BM-transplanted eNOS$^{-/-}$ mice but not in eNOS$^{-/-}$ control mice. (*B*) When values for EGFP$^+$ control heart and kidney were normalized to 1.0, we observed a three- to four-fold greater band intensity in control mice compared with BM-transplanted eNOS$^{-/-}$ mice. (*C*) The 500 bp band represents amplicons consisting of 450 bp of the disrupted exon 12 of the *eNOS* gene plus 50 bp of the targeting construct. The 450 bp band represents amplicons of the native *eNOS* gene. The label WT indicates amplicons of the wild-type *eNOS* gene and KO indicates amplicons of the knockout (*eNOS*$^{-/-}$) gene. (*C* and *D*) DNA banding patterns for the amplicons of native eNOS (450 bp) and EGFP (200 bp) in BM-transplanted mice indicated trace quantities present in both heart and kidney with high levels present in the reconstituted, haematopoietic spleen. No differences were observed when DNA from day-6, day-14 and day-28 transplanted mice was analysed. (*E* and *F*) EGFP mRNA expression was low in kidney and liver and high in the spleen, whereas expression of native eNOS mRNA was low in kidney, liver, and spleen. We believe the low-level eNOS mRNA expression in the spleen reflects the abundance of EGFP$^+$ WBC that are positive for eNOS DNA but do not express eNOS mRNA and protein. Mean $\pm$ SD; EGFP$^+$ controls, $n = 3$; BM-transplanted eNOS$^{-/-}$, $n = 4$; eNOS$^{-/-}$ controls, $n = 4$.

3.7 Confocal microscopy

Sections of heart, kidney, liver, and spleen from transgenic EGFP$^+$ control mice and BM-transplanted eNOS$^{-/-}$ recipients were stained with primary anti-EGFP and anti-SMαA antibodies and fluorophore-conjugated secondary antibodies. Endothelial cells in arteries of EGFP$^+$ control mice were consistently EGFP$^+$ (*Figure 3A–D*); however, no EGFP$^+$ endothelial cells were found in corresponding arteries in the chimeric BM-transplanted recipients (*Figure 3E–H*). The same labelling pattern was observed when aortas from transgenic and BM-transplanted eNOS$^{-/-}$ mice were examined (Supplementary material online, *Figures S1A and B*). No EGFP$^+$ endothelial cells were seen in the ascending and descending aorta of BM-transplanted eNOS$^{-/-}$ mice. Furthermore, terminal arterioles in heart, kidney, liver, and spleen did not show any evidence of incorporation of EGFP$^+$ endothelial cells (Supplementary material online, *Figure S2A–D*). In an additional effort to establish whether eNOS deficient endothelium can be renewed over time, we myeloablated WT mice using busulfan then transplanted EGFP$^+$ BM cells and reconstituted the recipient BM. One year after transplantation, organs were harvested and examined for endothelial cell renewal. No EGFP$^+$ endothelial cells were found in the lining of conducting arteries and arterioles in heart, kidney, and spleen (Supplementary material online, *Figure S3A–C*) at 1 year after transplantation. Thus, the endothelial linings of all arteries and arterioles examined in eNOS$^{-/-}$ mice, using multiple BM-transplanted protocols, remained devoid of EGFP$^+$ cells.

Sections of heart, kidney, liver, and spleen were prepared from transgenic EGFP$^+$ control mice and eNOS$^{-/-}$ BM

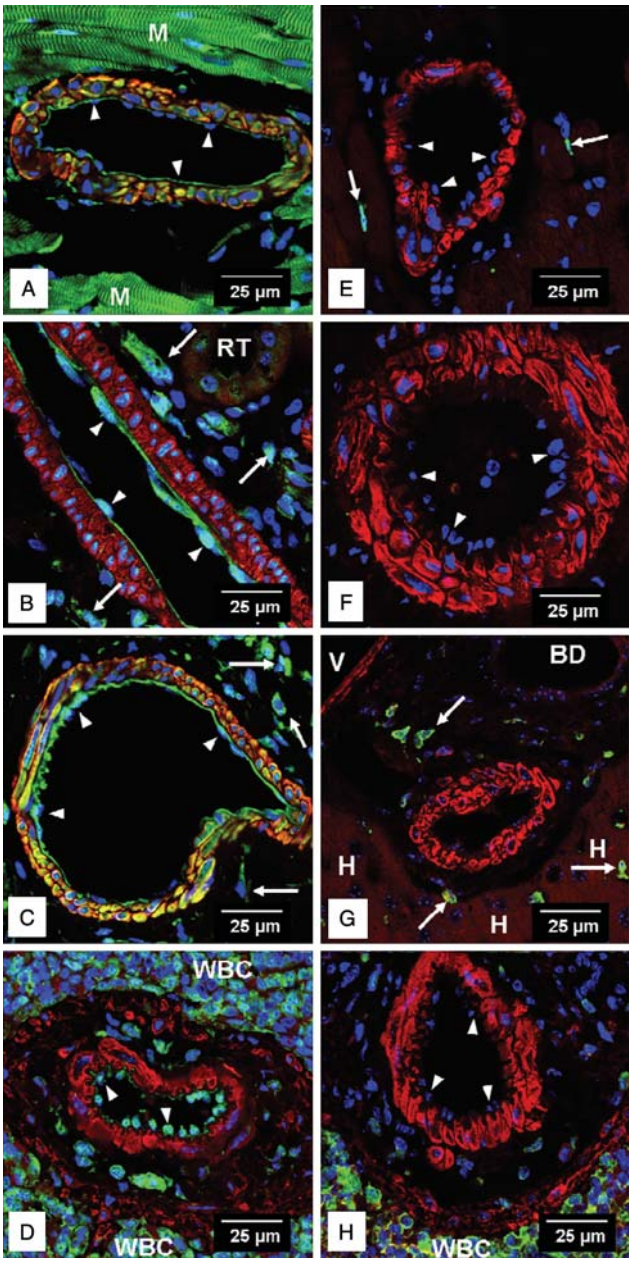

Figure 3 Confocal microscopy of conducting arteries in heart, kidney, liver, and spleen in EGFP$^+$ control mice are seen in (*A–D*). Arteries from corresponding organs in BM-transplanted eNOS$^{-/-}$ recipients are seen in (*E–H*). It is clear that all endothelial cells (arrowheads) in the coronary, renal, hepatic, and splenic arteries in the EGFP$^+$ control mice are EGFP$^+$ (green), whereas no EGFP$^+$ endothelial cells are found in arteries of BM-transplanted eNOS$^{-/-}$ mice. Several layers of smooth muscle cells are seen in the media layer (red) of these arteries. This pattern of labelling is consistently observed in all sections regardless of treatment protocol. Frequently, in areas near cardiomyocytes (M), renal tubules (RT), and hepatocytyes (H), EGFP$^+$ WBC are seen in capillaries and/or connective tissue (arrows). This is especially important in the BM-transplanted eNOS$^{-/-}$ mice (E–H) as a confirmation of maintained chimerism. In (G), a cross-section of a bile duct (BD) and a small portion of a portal vein (V) are seen. The splenic pulp is densely packed with EGFP$^+$ WBC (D and H). Green, EGFP; red, SMαA; yellow, merged EGFP and SMαA; blue, Nuclei.

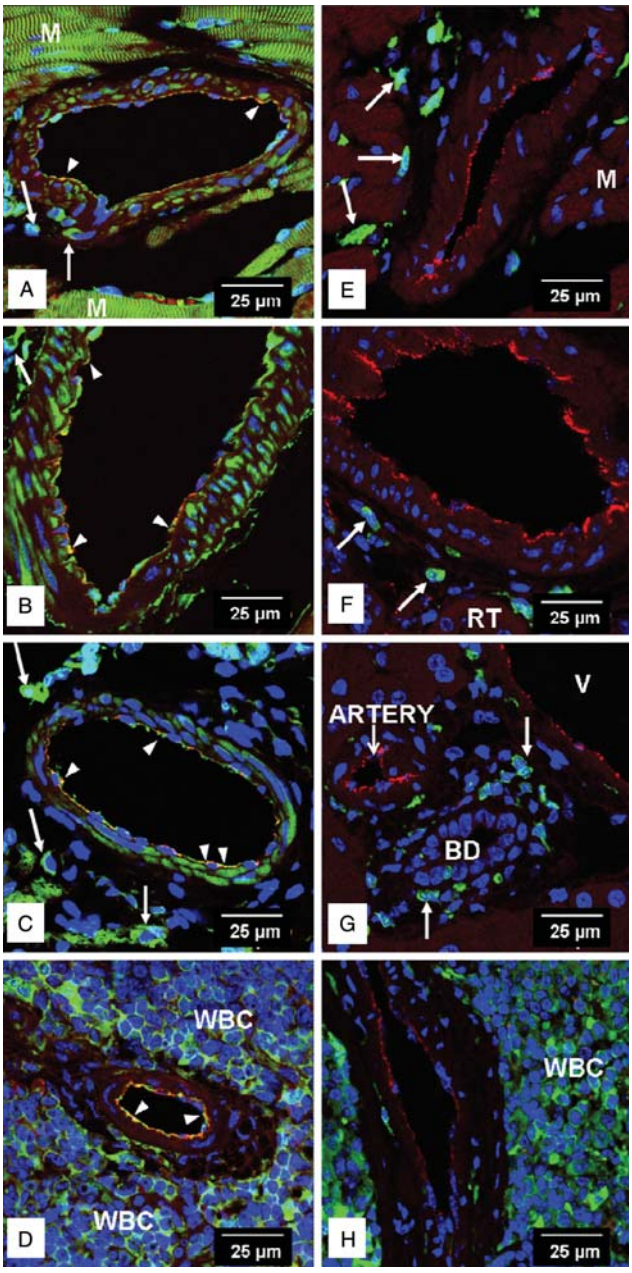

Figure 4 Confocal microscopy of conducting arteries in heart, kidney, liver, and spleen in EGFP$^+$ control mice are seen (*A–D*). Arteries from corresponding organs in BM-transplanted eNOS$^{-/-}$ recipients are seen (*E–H*). It is clear that all endothelial cells in the coronary, renal, hepatic, and splenic arteries in the EGFP$^+$ control mice are EGFP$^+$ (green), whereas no EGFP$^+$ endothelial cells are found in arteries of the BM-transplanted eNOS$^{-/-}$ mice. The sections were also stained with anti-vWF antibodies and all endothelial cells expressed vWF (red). Several layers of smooth muscle cells are seen in the media (green) of the arteries in EGFP$^+$ control mice. Endothelial cells in the coronary, renal, hepatic, and splenic arteries (A–D) are positive for EGFP and vWF. Merged images show yellow endothelial cells (arrowheads). The endothelium in the BM-transplanted eNOS$^{-/-}$ mice is positive only for vWF and appears red. Frequently, in areas near cardiomyocytes (M) and renal tubules (RT), EGFP$^+$ donor-derived WBC are seen in capillaries and/or connective tissue (arrows). This is especially important in the BM-transplanted eNOS$^{-/-}$ mice (E–H) as an indication of maintained chimerism. In (*F*), a small portion of a renal tubule (RT) is seen. In (*G*), a small portion of the portal vein (V) and bile duct (BD) are seen. The splenic pulp is densely packed with EGFP$^+$ WBC (D and H). Green, EGFP; red, vWF; yellow, merged EGFP and vWF; blue, Nuclei.

recipients that were irradiated and transplanted on day 6 or day 28. The sections were stained with primary anti-EGFP and anti-vWF antibodies and fluorophore-conjugated secondary antibodies. Endothelial cells in arteries were consistently positive for EGFP and vWF in transgenic donor mice (*Figure 4A–D*). Corresponding arteries in BM-transplanted eNOS$^{-/-}$ mice were typically devoid of EGFP$^+$ endothelial cells, but like the WT control mice were uniformly positive

for vWF (*Figure 4E–H*). We obtained these same results when the aorta and conductive arteries from transgenic controls and day-6 BM-transplanted eNOS$^{-/-}$ mice (Supplementary material online, *Figure S4A–C*) were analysed for EGFP and vWF expression. Collectively, these data indicate that the endothelial lining of arteries is intact in the eNOS$^{-/-}$ model as seen by the presence of vWF expression throughout the lining. However, these findings do not address the possibility that donor cells are incorporated into the endothelium but that EGFP expression is silenced in endothelial cells of transplanted eNOS$^{-/-}$ mice.

To control for possible silencing of the EGFP gene in our BM transplant protocols, we stained for eNOS expression in the endothelium of EGFP transgenic mice and eNOS$^{-/-}$ BM recipients. All endothelial cells in the aorta in transgenic donors expressed eNOS (*Figure 5A* and *C–E*), but there was no evidence for eNOS expression in the endothelial cells in aortas of BM-transplanted recipients (*Figure 5B*).

3.8 Alternate treatments to determine toxicity

To test for toxicity induced by radiation and BM transplantation, busulfan, a non-toxic myeloablative agent commonly used in BM transplant therapy, was substituted as a myeloablative agent prior to BM transplantation into eNOS$^{-/-}$ mice. We found no differences between busulfan-treated and radiation-treated mice (Supplementary material online, *Figures S1B and S3A–C*). Additionally, we transplanted day-6 and day-14 neonatal eNOS$^{-/-}$ mice, whose growth rates were accelerated compared with day-28-treated mice. There was no detectable evidence for EPC incorporation into vascular endothelium in neonatal mice or young adult mice when analysed for cardiovascular function by echocardiography, EGFP expression by molecular assays, or structure by confocal microscopy.

4. Discussion

There is a body of literature supporting the concept that BM-derived EPCs enter the circulation and contribute to postnatal angiogenesis, neovascularization, and endothelial cell renewal. We tested this concept in our study by asking whether BM-transplanted progenitor cells from a healthy donor might reconstitute the recipients BM and subsequently replace dysfunctional endothelium in an animal model with haemodynamic evidence of chronic endothelial dysfunction. We found no evidence to suggest that transplanted BM cells replaced dysfunctional arterial endothelium over time in an eNOS$^{-/-}$ mouse model of hypertension.

BM cells from healthy EGFP^{+} donors successfully reconstituted the BM of eNOS$^{-/-}$ mice when transplanted into sublethally irradiated mice on day 28 after birth. Four months after BM transplant, mean arterial pressure was not reduced in these eNOS$^{-/-}$ mice, suggesting that few if any EGFP^{+} eNOS^{+} donor-derived cells capable of producing nitric oxide had incorporated into recipient endothelium. Trace quantities of EGFP were detected by western blot in hearts and kidneys of BM-transplanted eNOS$^{-/-}$ mice compared with the control levels found in EGFP transgenic mice. Failure to identify EGFP^{+} endothelial cells in the arteries and arterioles of these BM-transplanted mice, by immunohistochemistry and confocal microscopy, suggested

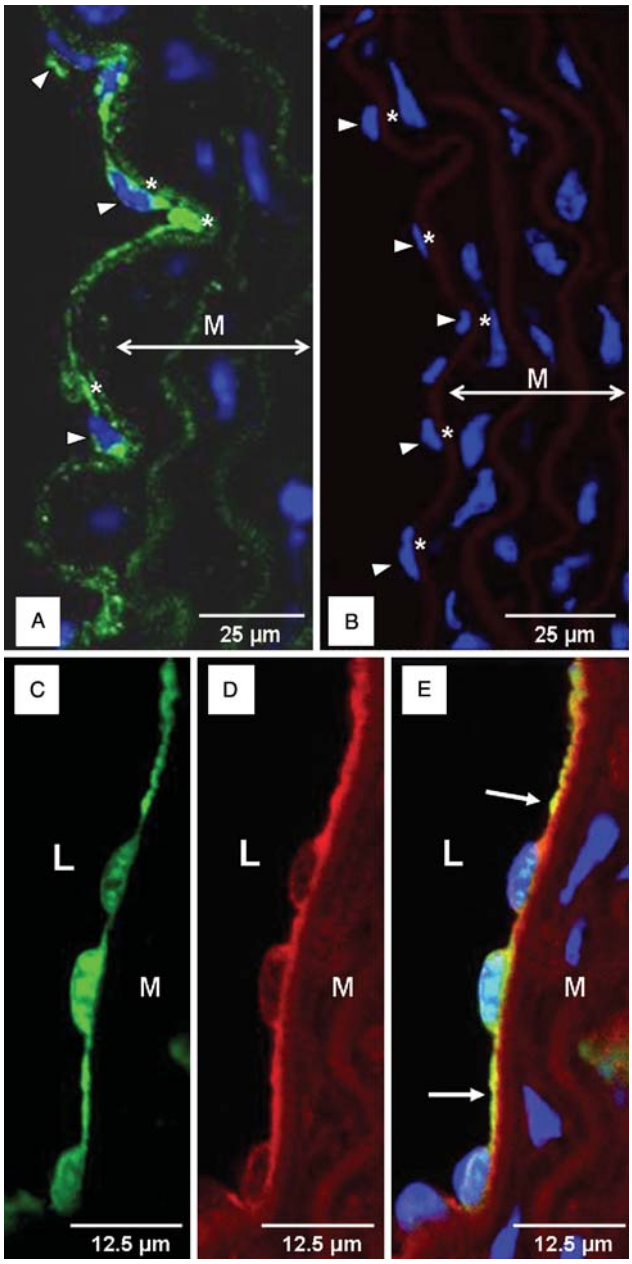

Figure 5 Confocal microscopic images of several aortas are seen in (*A–E*). The intima, which consists of a monolayer of endothelial cells, and the media (M) are seen in (A–E). Nuclei in the endothelial cells of control EGFP^{+} mice (A) are embedded in eNOS positive (green) cytoplasm (arrowheads) and lie on the underlying internal elastic membrane that displays a hint of green autofluorescence (*). In contrast, nuclei in endothelial cells in BM-transplanted eNOS$^{-/-}$ mice are 'bare' organelles (arrowheads) with no visible cytoplasm and appear to lie on the underlying internal elastic membrane (*) that displays a hint of (red) autofluorscence (B). In (A) and (B), green, eNOS; blue, nuclei. A portion of the endothelial and smooth muscle layers of the aorta of an EGFP^{+} control mouse is seen in (C–E). (E) In the merged image, the double positive endothelial cytoplasm is yellow (arrow). Green, EGFP; red, eNOS; yellow, merged EGFP and eNOS; blue, Nuclei.

to us that the low level of EGFP found in the hearts and kidneys of recipient mice by western blot or DNA analysis was contributed by residual WBCs in the circulation following total body PBS perfusion and by WBCs in surrounding extravascular connective tissue sites. We found support for this interpretation by quantitative RT–PCR analysis of eNOS expression in organs of recipient mice. eNOS mRNA,

highly expressed in EGFP$^+$ mice, was not readily detected in organs of BM-transplanted eNOS$^{-/-}$ mice. Presumably, the mature, circulating EGFP$^+$ blood cells in kidney and liver produced little or no eNOS mRNA. Likewise, the numerous developing and re-circulating mature EGFP$^+$ blood cells in splenic haematopoietic tissue expressed no detectable eNOS mRNA.

Contrary to the widely held concept that BM-derived, circulating EPCs contribute to postnatal angiogenesis and neovascularization, several recent reports claim that BM is not a source of EPCs in arteriosclerotic grafts or in response to hind-limb ischaemia.[16,17] Our data support these novel findings, in this highly controversial field, by demonstrating a lack of BM-derived endothelial cell incorporation into the lining of the dysfunctional endothelium in eNOS$^{-/-}$ mice during a 4 month period following BM transplantation. However, we observed EGFP$^+$ cells near the outer arterial wall of many vessels and within the adventitial layer, but we did not assess whether these BM-derived EGFP$^+$ cells were pericytes or monocytes engaged in paracrine secretions as suggested by others.[18–25] According to this hypothesis, pericytes or monocytes that reside within the adventitia or occupy a vasculogenic zone at the interface of the smooth muscle and adventitial layers of the artery may monitor the behaviour of vasculogenic cells that reside within the vessel wall.[25–27] This observation merits additional investigation.

We considered the possibility that sub-lethal radiation followed by BM transplantation was toxic to the eNOS$^{-/-}$ mice in our study. Although this possibility cannot be fully excluded, we did not find evidence that radiation followed by BM transplantation induced any long-term negative effects. There was no decrease in body weight among the BM-transplanted eNOS$^{-/-}$ mice compared with non-transplanted eNOS$^{-/-}$ controls, and their physical activity level was equal to that of the non-transplanted eNOS$^{-/-}$ mice and WT controls. Additionally, when busulfan, a non-toxic myeloablative agent commonly used during BM transplants in children, was substituted for radiation therapy, we found no difference in cardiovascular structure and function between these mice and the radiation-treated day-28 mice.

To further evaluate transplant protocols that might product benefit through endothelial renewal, we treated day-6 and day-14 neonatal eNOS$^{-/-}$ mice, whose growth rate and vascular expansion are accelerated in comparison with day-28 transplanted mice, with sub-lethal radiation and BM transplant. No detectable improvements in outcome were observed when these younger mice were compared with the older day-28-treated mice.

Our findings differ from those of an earlier study by Guthrie *et al.*[28] in which GFP$^+$ BM was transplanted into adult eNOS$^{-/-}$ mice following laser-induced retinal injury. In this mouse model, EGFP$^+$ BM-derived cells gave rise to retinal vasculature and, importantly, to EGFP$^+$ endothelium in non-injured arteries in brain, thymus, and spleen. This study and ours utilized eNOS$^{-/-}$ C57BL/6J mice and sub-lethal radiation (6–6.5 Gy). Guthrie *et al.* enriched and injected 2500 Sca-1$^+$ c-kit$^+$ lin$^-$ EGFP$^+$ BM cells, whereas we injected $25 \times 10e^7$ nucleated BM cells in which the Sca-1$^+$ c-kit$^+$ lin$^-$ phenotype occurs at a ratio of 1:100 000. Thus, both studies utilized 2500 EGFP$^+$ primitive BM cells. In one major difference, photoagglutination of the retinal vasculature may have produced an inflammatory or cytokine response leading to systemic endothelial cell damage and renewal. In our study, no injury was inflicted during the time interval between sub-lethal radiation, BM transplant, and tissue analysis. In another major difference, Guthrie *et al.* stained 10 μm cryopreserved sections for confocal microscopy, whereas we examined 5 μm formalin fixed and paraffin embedded sections. The 5 μm formalin fixed sections provide greater resolution. We believe our protocol, which lacks induced vascular injury, may provide useful pre-clinical data regarding the inability of EPCs to renew endothelium in a setting of chronic endothelial cell dysfunction and hypertension.

The BM transplant protocol was successful and the mice in our study group showed blood cell chimerism greater than 85%. However, we did not find evidence for incorporation of BM-derived EGFP$^+$ cells into arterial or arteriolar endothelium, nor were we able to improve hypertension in BM-transplanted eNOS$^{-/-}$ mice. Hence, we conclude that BM-derived cells, if they enter the circulation as EPCs, do not participate in endothelial homeostasis and thus do not repair chronic, systemic endothelial dysfunction in young mice.

Supplementary material

Supplementary material is available at *Cardiovascular Research* online.

Acknowledgements

Special thanks to the staff of the Mouse Imaging Facility (NINDS, NIH), the Building 10A Animal Facility (NIH), the Confocal Microscope Core Facility (NHLBI, NIH), and the Flow Cytometry Core Facility (NHLBI, NIH) for access to the equipment.

Conflict of interest: none declared.

Funding

This work was supported by the intramural research program of the NHLBI, National Institutes of Health, Bethesda, MD, USA. Funding to pay the Open Access charges was provided by the NHLBI, National Institutes of Health.

References

1. Shepherd RM, Capoccia BJ, Devine SM, DiPersio J, Trinkaus KM, Ingram D *et al.* Angiogenic cells can be rapidly mobilized and efficiently harvested from the blood following treatment with AMD3100. *Blood* 2006;**108**: 3662–3667.
2. Hill JM, Zalos G, Halcox JPJ, Schenke WH, Waclawiw MA, Quyyumi AA *et al.* Circulating endothelial progenitor cells, vascular function, and cardiovascular risk. *N Engl J Med* 2003;**348**:593–600.
3. Asahara T, Masuda H, Takahashi T, Kalka C, Pastore C, Silver M *et al.* Bone marrow origin of endothelial progenitor cells responsible for postnatal vasculogenesis in physiological and pathological neovascularization. *Circ Res* 1999;**85**:221–228.
4. Shi Q, Rafii S, Wu MH, Wijelath ES, Yu C, Ishida A *et al.* Evidence for circulating bone marrow-derived endothelial cells. *Blood* 1998;**92**:362–367.
5. Takahashi T, Kalka C, Masuda H, Chen D, Silver M, Kearney M *et al.* Ischemia- and cytokine-induced mobilization of bone marrow-derived endothelial progenitor cells for neovascularization. *Nat Med* 1999;**5**: 434–438.
6. Aicher A, Heeschen C, Mildner-Rihm C, Urbich C, Ihling C, Technau-Ihling K *et al.* Essential role of endothelial nitric oxide synthase for mobilization of stem cells and progenitor cells. *Nat Med* 2003;**9**: 1370–1376.

7. Orlic D, Kajstura J, Chimenti S, Limana F, Jakoniuk I, Quaini F *et al*. Mobilized bone marrow cells repair the infarcted heart, improving function and survival. *Proc Natl Acad Sci* 2001;**98**:10344–10349.
8. Askari AT, Unzek S, Popovic ZB, Goldman CK, Forudi F, Kiedrowski M *et al*. Effect of stromal-cell-derived factor-1 on stem-cell homing and tissue regeneration in ischaemic cardiomyopathy. *Lancet* 2003;**362**:697–703.
9. Ceradini DJ, Kulkarni AR, Callaghan MJ, Tepper OM, Bastidas N, Kleinman ME *et al*. Progenitor cell trafficking is regulated by hypoxic gradients through HIF-1 induction of SDF-1. *Nat Med* 2004;**10**:858–864.
10. Zentilin L, Tafuro S, Zacchigna S, Arsic N, Pattarini L, Sinigaglia M *et al*. Bone marrow mononuclear cells are recruited to the sites of VEGF-induced neovascularization but are not incorporated into the newly formed vessels. *Blood* 2006;**107**:3546–3554.
11. Li T-S, Hamano K, Nishida M, Hayashi M, Ito H, Mikamo A *et al*. CD117+ stem cells play a key role in therapeutic angiogenesis induced by bone marrow cell implantation. *Am J Physiol* 2003;**285**:H931–H937.
12. Nakano M, Satoh K, Fukumoto Y, Ito Y, Kagaya Y, Ishii N *et al*. Important role of erythropoietin receptor to promote VEGF expression and angiogenesis in peripheral ischemia in mice. *Circ Res* 2007;**100**:662–669.
13. Elsheikh E, Uzunel M, He Z, Holgersson J, Nowak G, Sumitran-Holgersson S. Only a specific subset of human peripheral-blood monocytes has endothelial-like functional capacity. *Blood* 2005;**106**: 2347–2355.
14. Lin Y, Weisdorf DJ, Solovey A, Hebbel RP. Origins of circulating endothelial cells and endothelial outgrowth from blood. *J Clin Invest* 2000; **105**:71–77.
15. Shesely EG, Maeda N, Kim HS, Desai KM, Krege JH, Laubach VE *et al*. Elevated blood pressures in mice lacking endothelial nitric oxide synthase. *Proc Natl Acad Sci USA* 1996;**93**:13176–13181.
16. Hillebrands JL, Klatter FA, van Dijk WD, Rozing J. Bone marrow does not contribute substantially to endothelial-cell replacement in transplant arteriosclerosis. *Nat Med* 2002;**8**:194–195.
17. Aicher A, Rentsch M, Sasaki K, Ellwart JW, Fandrich F, Siebert R *et al*. Nonbone marrow-derived circulating progenitor cells contribute to postnatal neovascularization following tissue ischemia. *Circ Res* 2007;**100**: 581–589.
18. O'Neill TJ, Wamhoff BR, Owens GK, Skalak TC. Mobilization of bone marrow-derived cells enhances the angiogenic response to hypoxia without transdifferentiation into endothelial cells. *Circ Res* 2005;**97**: 1027–1035.
19. Sahara M, Sata M, Morita T, Nakamura K, Hirata Y, Nagai R. Diverse contribution of bone marrow-derived cells to vascular remodeling associated with pulmonary arterial hypertension and arterial neointimal formation. *Circulation* 2007;**115**:509–517.
20. Ziegelhoeffer T, Fernandez B, Kostin S, Heil M, Voswinckel R, Helisch A *et al*. Bone marrow-derived cells do not incorporate into the adult growing vasculature. *Circ Res* 2004;**94**:230–238.
21. Purhonen S, Palm J, Rossi D, Kaskenpaa N, Rajantie L, Yla-Herttuala S *et al*. Bone marrow-derived endothelial precursors do not contribute to vascular endothelium and are not needed for tumor growth. *Proc Natl Acad Sci* 2008;**105**:6620–6625.
22. Rehman J, Li J, Orschell CM, March KL. Peripheral blood 'endothelial progenitor cells' are derived from monocytes/macrophages and secrete angiogenic growth factors. *Circulation* 2003;**107**:1164–1169.
23. Yoder MC, Mead LE, Prater D, Krier TR, Mroueh KN, Li F *et al*. Redefining endothelial progenitor cells via clonal analysis and hematopoietic stem/progenitor cell principals. *Blood* 2007;**109**:1801–1809.
24. Hur J, Yang HM, Yoon CH, Lee CS, Park KW, Kim JH *et al*. Identification of a novel role of T cells in postnatal vasculogenesis. *Circulation* 2007;**116**: 1671–1682.
25. Ingram DA, Mead LE, Moore DB, Woodard W, Fenoglio A, Yoder MC. Vessel wall-derived endothelial cells rapidly proliferate because they contain a complete hierarchy of endothelial progenitor cells. *Blood* 2005;**105**: 2783–2786.
26. Alessandri G, Girelli M, Taccagni G, Colombo A, Nicosia R, Caruso A *et al*. Human vasculogenesis ex vivo: embryonal aorta as a tool for isolation of endothelial cell progenitors. *Lab Invest* 2001;**81**:875–885.
27. Zengin E, Chalajour F, Gehling UM, Ito WD, Treede H, Lauke H *et al*. Vascular wall resident progenitor cells: a source for postnatal vasculogenesis. *Development* 2006;**133**:1543–1551.
28. Guthrie SM, Curtis LM, Mames RN, Simon GG, Grant MB, Scott EW. The nitric oxide pathway modulates hemangioblast activity in adult hematopoietic stem cells. *Blood* 2005;**105**:1916–1922.